Research Square

Preprints are preliminary reports that have not undergone peer review.
They should not be considered conclusive, used to inform clinical practice,
or referenced by the media as validated information.

Organic-Inorganic Hyphenated Beads Supporting Co-adsorption of Congo Red and Crystal Violet dyes: Studies on Composition Flip-Flop and Crosslinking Effects

Arundhati Chakraborty
University of Calcutta
Sonai Dutta
University of Calcutta
Reetika Sarkar
University of Calcutta
Debasis Brahma
University of Calcutta
Anirban Mukherjee
Gurudas College, University of Calcutta
Amit Sen
Hari Shankar Singhania Elastomer and Tyre Research Institute, Hebbal Industrial Estate
Prasenjit Ghosh
Hari Shankar Singhania Elastomer and Tyre Research Institute, Hebbal Industrial Estate
Rabindra Mukhopadhyay
Hari Shankar Singhania Elastomer and Tyre Research Institute, Hebbal Industrial Estate
Suman Acharya
Indian Rubber Materials Research Institute
Debdipta Basu
Indian Rubber Materials Research Institute
Arjun Maity
University of South Africa
Abhijit Bandyopadhyay
abpoly@caluniv.ac.in

University of Calcutta

Research Article

Keywords: Beads, Dye, Co-Adsorption, Chitosan, Kaolin

Posted Date: August 20th, 2026

DOI: https://doi.org/10.21203/rs.3.rs-10343464/v1

License: This work is licensed under a Creative Commons Attribution 4.0 International License.
Read Full License

Additional Declarations: No competing interests reported.

Abstract

This work involves the strategic design and fabrication of novel hybrid beads, consisting of an organic and an inorganic layer for co-adsorption of Congo Red (CR) and Crystal Violet (CV) dyes from a binary mixture. A series of hybrid biopolymer-based adsorbents having variable compositions was synthesised by crosslinking Chitosan (CS) with Glutaraldehyde (GL) and embedding Kaolin (kao), followed by surface grafting with 2-Hydroxyethyl Methacrylate (HEMA) monomers. Among the multiple adsorbents tested, one of the optimised hybrid formulations (AC-20) with 79.3% crystallinity was found to effectively co-adsorb 99.7% of CR and 95.4% of CV simultaneously from a binary mixture of 10 ppm strength at pH 1 in 4 hours at a temperature of 313 K using an adsorbent dosage of 0.05 g/10 mL. Effective dye removal was retained even at pH=3 leading to 84.9% CR and 91.9% CV removal from binary dye mixture. Several characterisation techniques, including FTIR analysis, swelling studies, zeta potential analysis, UV-visible spectroscopy, SEM-EDX and XRD analysis, were performed. Kinetic modelling described that CR (R^2=0.997) and CV (R^2=0.996) adsorption followed the pseudo-second-order model. This study successfully addresses both environmental hazards and practical wastewater treatment needs by using the eco-friendly adsorbent beads as a promising solution for real-world remediation of toxic dye mixtures.

Introduction

Water is universally recognised as a vital resource underpinning all forms of terrestrial life. Availability of sufficient amounts of freshwater to support all life on earth has been a major concern, especially for a densely populated country like India. Urbanisation, rapid industrial growth and climate change have increased the need of preserving and treating water in order to reduce the water crisis. The textile, dye, paint, varnish, paper, tannery, and pharmaceutical manufacturing industries are the major contributors of water pollutants. A recent estimate revealed that annually, around 70 lakh tons of dye are produced worldwide.[1] The production of paper, printing and textile dyes releases approximately 10–15% of the organic dyes in the environment. Since these dyes are usually carcinogenic throughout the food chain and can seriously endanger human health and aquatic life even in trace amounts, it is imperative that they are disposed of properly.[2] In the last 25–30 years, dye production as well as export in Asian countries like India and China has increased significantly, thus a wide growth of these industries is observed in recent times.[3] Although it is a boon for the economy of developing countries like India, it also has many adverse environmental impacts, as the discharge of industrial wastewater containing harmful dyes into the water bodies leads to their accumulation without degradation and remains intact for a long period in the environment, which contaminates the groundwater sources. It is a serious threat to the environment and includes severe harm to aquatic plants and organisms because of their strong colour and bio-recalcitrant components.[12] Dyes also have several harmful impacts on human beings and affect vital organs like the brain, kidney, heart and liver.[4] The most important dye pollutants are Congo Red, Crystal Violet, Methyl Orange, Methylene Blue, etc.CR is an anionic dye with the SO_3^- group in its primary structure and has a pKa value of 4.5. It also belongs to the category of azo-based dyes; the

azo linkage gives them extra stability against light, heat and aerobic degradation. [2, 5] Even a minute quantity of CR dye can cause considerable damage to aquatic environments by reducing the oxygen level of water.[2] CR causes gastrointestinal irritation, mutation, lung and bladder cancer, gene mutation in human beings, and thus it is considered the most harmful and most widely used dye. It is extensively used for dyeing paper and textiles, including silk, cotton, hemp, rubber, and cosmetics.[6] CV is a cationic triphenylmethane dye and is responsible for causing irritation to the eyes, skin and digestive tract. It acts as a mitotic poisoning agent and is thus regarded as a potential biohazard because of its non-biodegradability. [7,8]

Wastewater has been treated by a variety of approaches and strategies, including coagulation, flocculation, sedimentation, filtering, and adsorption for more than a century at different stages of the water treatment process. Although traditional wastewater treatment methods like flocculation and coagulation were found to be successful in removing pollutants from wastewater, they pose a serious risk of contaminating the environment and have high operational cost.[10, 16] Adsorption is the most versatile water treatment technology because it is straightforward, simple to design, eco-friendly and sustainable way of removing numerous pollutants including industrial dyes, heavy metals and pharmaceutical wastes from wastewater at low operational cost.[15]Accordingly, the focus is to develop green, environment friendly adsorbents with high aptitude for adsorption. Natural polymers like chitosan, guar gum, pectin, alginates, etc. are effective candidates for developing adsorbents in a sustainable manner as they are environment friendly, easily available, low-cost, and environmentally benign.[13]CS, which is N-deacetylated chitin, is the second most abundant biopolymer after Cellulose.[9] It is considered the main component of the shells of crabs, shrimp, prawns, and krill [14] and is a naturally abundant polysaccharide with the presence of a significant number of reactive amino and hydroxyl functionalities in its structure, which enables CS to act as an efficient adsorbent. India is one of the major commercial producers of CS, and thus it is easily available as well as a cost-effective biopolymer. [11] Pure CS has a low surface area and limited mechanical stability, and poor adsorption kinetics.[15] Crosslinking of CS was needed for enhancing the mechanical strength, chemical stability and improving the adsorption ability of CS based adsorbents.[17, 18] Grafting of monomers onto the polymer matrix improves its properties as it incorporates additional functional groups into the base polymer matrix.[19] Inorganic Clays, hydrated aluminosilicates are widely available, abundant, cost-effective, environment friendly material which plays an effective role as adsorbents because it provides high stability, large surface area, owing to its layered structure and good bonding ability due to the presence of a large number of hydroxyl groups on the surface.[20, 21] Thus, we aimed to incorporate the properties of both inorganic clay and organic polysaccharide in the form of a hyphenated bead-like adsorbent. Mohamed M. Abou Alsoaud developed kaolin-impregnated aminated chitosan composite beads for the adsorption of anionic CR dye.[15] Vanderlane Cavalcanti Silva explored the ability of heat treated Brazilian palygorskite to remove CV and CR dyes and found 98% removal of both the dyes at basic pH in 360 minutes.[22] Salma Ssouni observed that chitin could successfully remove 99.47% CV dye and 82.15% for the CR dye at a pH of 12 for CV and 2 for CR in 90 minutes.[61] Developing adsorbents in the form of beads was done by Meriem Fizir using alginate and kaolin, and the beads were found to be effective in

recovering phosphate from domestic and hydroponic wastewater.[23] CS-clay based adsorbent in the form of beads was developed by Shanta Biswas, which had a promising adsorption performance towards Cr (VI) and Pb (II) ions and methylene blue dye.[24]Beads possess enhanced robustness and resist fragmentation even post adsorption, which enables their regeneration by suitable desorption techniques. Developing adsorbents in the form of beads not only enhances their adsorption efficiency but also provides a prospect towards devising a fixed bed column which has the potential to offer continuous contaminant removal from wastewater and efficient process automation, establishing them as an ideal solution for real-world wastewater treatment, which is advantageous from an industrial point of view as well.[25]

Most of the previous studies focused on physical blending between polysaccharides and clay particles, leading to a random dispersion of the particles. The majority of documented systems depend on uniformly mixing inorganic fillers into an organic polymer matrix, which frequently results in low interfacial compatibility and restricted adsorption selectivity. To get over these restrictions, the current study offers a structurally layered hybrid bead architecture, which is a significant shift from conventional composite fabrication. Here, we have aimed to incorporate the essential features of both organic and inorganic counterparts in a spherical bead-like form with improved surface area, which enhanced the adsorption efficiency. The development of adsorbents in the form of a bead was purposefully made as it facilitates easier separation of adsorbents from treated solution post adsorption processes, thus overcoming the challenges associated with retrieving fine, dispersed adsorbent particles. The development of CS-clay beads with grafted monomers for co-adsorption of cationic and anionic dyes from their binary mixture was scarcely explored. Unlike traditional blend-type composites, the novelty of our work lies in the layered structure of the hyphenated beads with a distinct separation between the inorganic clay and organic polysaccharide layers. The hyphenated beads could be tailored by varying the kao content. A well-defined contrast in structure and surface morphology was observed with proportional variation of organic and inorganic counterparts, leading to a precise localisation of inorganic and organic domains within a single bead. Our work aimed to synthesise beads where a unique flip-flop between the organic and inorganic layers over the surface could be achieved by composition variation, which was essential for controlling the surface chemistry of the beads. The developed CS-kao beads were used for co-adsorptive removal of a binary mixture of noxious cationic and anionic dyes.CR and CV were chosen as anionic and cationic dyes because of their widespread usage, distinct structure, environmentally persistent and toxic characteristics, which cause substantial damage to aquatic life as well as human health. Together, CR and CV could represent the typical anionic and cationic contaminants which are very often present in the industrial effluents and thus their binary mixture is an ideal model system for performing dye removal studies under realistic, complex multi-dye containing wastewater, where co-adsorption of anionic and cationic colours by using a single adsorbent is essential. However, most of the pre-existing studies focus on single dye or selective dye adsorption. Co-adsorption of cationic and anionic dyes from their binary mixture is not yet widely explored. Our work was directed to target real-world wastewater problems where a mixture of dyes with variable nature could be removed at the same operational pH by co-adsorption using a single adsorbent. The resultant

beads demonstrate their suitability for the co-removal of oppositely charged dyes in complicated industrial effluents due to their exceptional adsorption effectiveness, stability, and reusability under a range of pH levels. The present study also provides novel insights into sequential dye adsorption mechanisms for a mixed dye system and demonstrates strong potential for usage in fixed-bed continuous flow columns.

Experimental

2.1 Materials:

CS from Shrimp Shells 75% (deacetylated) was purchased from Loba Chemie Pvt. Ltd., kao was obtained from B.D. Pharmaceuticals Works Pvt. Ltd. Howrah, West Bengal, India, GL 25% solution in water was purchased from Merck Life Science Private limited, HEMA 96.5% Extra Pure was purchased from Loba Chemie, Potassium peroxodisulphate (KPS) extra pure from Merck Life Science Private Limited, Acetic acid glacial 99–100% and sodium hydroxide pellets from Merck Life Science Private Limited, Milli Q water were used for the synthesis of hyphenated crosslinked beads grafted by HEMA. CR and CV dye powders from Nice Chemicals were used for the preparation of model wastewater.

2.2 Synthesis of crosslinked CS-kao beads:

250 mg of CS flakes was dissolved in 2% acetic acid solution. It was followed by the addition of kao in various proportions to prepare 1:0.5, 1:1 and 1:2 Cs-kao homogeneous solutions, along with the addition of GL (used as crosslinker) into the homogeneous solution, followed by mechanical stirring for 1.5 hours at room temperature. The slurry was added dropwise to a 1 (M) NaOH solution for bead formation using a plastic syringe.[26] The excess NaOH was removed by washing the beads with deionised water. A total of six variants of crosslinked beads (CSK) were synthesised by stoichiometric variation as detailed in Table 1 and were air dried.

Table 1
Sample composition of crosslinked CSK beads by varying the amount of Kao and GL:

CS: Kao	**1:0.5**	**1:0.5**	**1:1**	**1:1**	**1:2**	**1:2**	**1:0**
GL (mmol)	0.847	15	0.847	15	0.847	15	15
Designation	CSK1	CSK 2	CSK 3	CSK 4	CSK 5	CSK 6	CSK 7

2.3. Synthesis of HEMA grafted beads:

The previously synthesised CSK beads (150 mg) were taken, followed by the addition of 3% KPS solution under a nitrogen atmosphere at 70℃ to initiate free radical formation. After 20 minutes, HEMA was added slowly, and the reaction was allowed to continue for 4 hours under a nitrogen atmosphere.[27] The grafted beads were washed with distilled water to remove unreacted monomers. They were air-dried

before characterisation. A total of eighteen variants of grafted beads were synthesised as detailed in Table 2.

Table 2
Sample composition of grafted beads by varying the amount of HEMA:

Designation	CSK variants	HEMA (mmol)
AC-25	CSK 1	0.57
AC-28	CSK 1	1.14
AC–24	CSK 1	1.71
AC-30	CSK 2	0.57
AC-29	CSK 2	1.14
AC-26	CSK 2	1.71
AC-3	CSK 3	0.57
AC-2	CSK 3	1.14
AC-14	CSK 3	1.71
AC–20	CSK 4	0.57
AC-12	CSK 4	1.14
AC-13	CSK 4	1.71
AC-4	CSK 5	0.57
AC-27	CSK 5	1.14
AC–16	CSK 5	1.71
AC-22	CSK 6	0.57
AC-23	CSK 6	1.14
AC-21	CSK 6	1.71
AC-1	CSK 7	0.57

2.4 Preparation of model wastewater:

Textile industry wastewater contains a complex mixture of hazardous dyes that pose significant environmental and health risks. Among these, CR, an anionic diazo dye, and CV, a cationic triarylmethane dye, are major pollutants and are chosen as model dyes. To prepare model wastewater for controlled adsorption experiments, a 500 mL stock solution containing 10 ppm each of CR and CV was prepared using a volumetric flask to ensure accuracy. The pH of the dye mixture solutions was systematically

varied using 0.1 N HCl and 0.1 N NaOH to investigate the influence of solution pH on adsorption behaviour.

2.5 Batch adsorption:

The synthesised beads (0.05 g) were added to 10 mL of CR and CV dyes individually, as well as in their binary mixture solutions (10 ppm each), taken in a 100 mL conical flask, while the pH was adjusted in the range of 1–11 using 0.1 M HCl and 0.1 M NaOH solutions. Batch adsorption studies were performed by continuously stirring in a shaker for 4 hours. After filtration, the resulting solutions were collected, and the concentration of residual CR and CV dyes were measured using UV-Visible spectrophotometry. For individual dyes, maximum absorbance was obtained at 497 nm for CR [28] and 589 nm for CV [29]. But for binary dye mixtures, individual λ_{max} values of both the dyes could not be obtained separately due to the overlapping of the two peaks. Thus, deconvolution of the UV-Vis spectra was performed using Origin Pro 9 software in order to find out two separate peaks for the respective dyes and their absorbance values were recorded. A shift in λ_{max} values was observed, which indicated strong interactions between the cationic and anionic dyes in the binary mixture. The adsorption capacity was measured in terms of percentage removal (R %) using the Eq. 1:[30]

$$R\ \% = \frac{C_0 - Cf}{C_0} \times 100 \text{ ----------(1)}$$

Where C_0 is the initial concentration of the binary mixture solution (10 mg/L), and C_f is the residual dye concentration after adsorption in mg/L. The concentration of the dye solution was obtained by calibration of the UV plot.

2.6 Characterisation:

2.6.1 Characterisation of adsorbents:

2.6.1.1 Fourier transform infrared (FTIR) spectroscopy:

FTIR spectroscopy of neat CS, non-grafted and grafted adsorbent beads (before and after dye adsorption) was carried out using a Perkin Elmer FTIR Spectrum Two spectrophotometer, covering the spectral range of 400 – 4000 cm^{-1} with a peak resolution of 4 cm^{-1}. The measurements were conducted in attenuated total reflectance mode using a diamond crystal to find out the chemical structure of the adsorbent beads.

2.6.1.2 Measurement of Zeta Potential:

A zeta potential analyser (model: ZEN3600, Serial No: MAL 1032012) purchased from Malvern Instruments Limited, U.K., Malvern Instruments Limited used for surface charge determination of the adsorbents before and after adsorption. The samples were prepared as 0.5% aqueous solutions and tested at room temperature.

2.6.1.3 Swelling Capacity determination:

The swelling behaviour of the prepared adsorbent beads was analysed by immersing the beads in 10 mL of distilled water. At certain specific time intervals, the samples were removed from water and gently dabbed on a tissue paper to remove excess water and weighed using an electronic balance (Model: MK 20E, Adair Dutt, India; readability: 0.1 mg). The water uptake was calculated from the difference between the weights of the final swollen and initial dry beads. The swelling percentage was measured in terms of the Eq. 2:[31]

Swelling % = $\frac{w_2 - w_1}{w_1} \times 100$ ----------(2)

where w_2 is the mass of the swollen bead, and w_1 is the mass of the dried bead before immersing it in water.

2.6.1.4 Scanning Electron Microscopy–Energy Dispersive X-ray spectrometry (SEM-EDX):

In order to investigate the surface morphology of beads containing variable amounts of kaolin and elemental analysis of the adsorbent beads before and after adsorption, SEM-EDX analysis was performed using FESEM – Make: Thermoscientific, Model: Apreo-S instrument.

2.6.1.5 X-Ray Diffraction Analysis:

The crystallinity of the samples was analyzed using a PANalytical X'pert PRO MRD x-ray diffractometer (40kV, 40mA) with Cu Kα radiation (wavelength = 1.5406Å) and at a scan rate of 2°per minute. The samples were scanned over a range of 2θ: 10°- 70°.

2.6.2 Characterisation of model wastewater containing a binary mixture of CR and CV dyes:

The UV-Visible spectrophotometer model LI-296 (Microprocessor UV-VIS Single Beam) from Lasany was used to measure the absorbance of the binary mixture of the dyes after adsorption at room temperature using a quartz cuvette with quartz slits and a 10 mm path length. The cuvette was rinsed with deionised water, followed by rinsing it with 0.1 N HCl or 0.1 N NaOH solutions as the dye samples were prepared at acidic and basic conditions, respectively. This was repeated after each cycle. It was filled with deionised water as a reference and baseline correction was done in the absence of any sample. Approximately 2 mL of solution was introduced into the cuvette, and absorbance was measured. The scan range was set between 800 nm and 200 nm.

2.7 Adsorption Kinetics Studies:

At certain specific time intervals, a 2 mL aliquot was withdrawn from the aqueous solutions of the binary dye mixture and the concentration of both CR and CV was found out by deconvolution of the obtained UV spectra, followed by calibration. Kinetics of the dye adsorption were investigated by fitting the data to various kinetic models (pseudo-first order, pseudo-second order, second order and intraparticle diffusion

models. The most appropriate model was analysed by comparing the R^2 values of the various curves. The adsorption capacity q_t (mg/g) was measured according to the Eq. 3: [15]

$$q_t = \frac{(c_0 - c_t)}{w} \times V \text{ ----------(3)}$$

q_t (mg/g) is the amount of dye adsorbed in time t (mins), c_0 is the initial concentration of dye mixture solution in mg/L, and c_t is the final concentration of dye solutions after adsorption in mg/L, V is the volume of solution in L, and w is the dosage of adsorbent in g.

Results and Discussions

3.1 Synthesis of Kaolin-CS grafted beads:

In order to improve the solubility of CS, it was made to dissolve in acetic acid solution where the amino groups of CS underwent protonation, thereby facilitating its dissolution.[32] Kaolin, a layered aluminosilicate clay, features abundant surface hydroxyl groups that not only participate in hydrogen bonding and other non-covalent type interactions with dye molecules but also form strong interactions with the CS matrix.[33] Since beads without kao were found to be comparatively more fragile, the addition of kao gave the CS beads structural support and preserved their spherical shape, significantly increasing their mechanical strength. The AC-1 beads were unable to demonstrate enough dye removal from their binary mixture, which further highlighted the significance of inorganic clay along with polysaccharide in bead production (Figure S1 and S2). Functionally, kao significantly augmented the adsorption capacity of the beads, contributing both surface-active sites for direct dye binding and elevating the total surface area for dye penetration and diffusion. The adsorption process was governed by a variety of non-covalent interactions, such as hydrogen bonding, van der Waals forces, hydrophobic interactions, stacking interactions and electrostatic interactions depending on the pH conditions, where the surface charges of both kao and CS facilitated multi-modal dye capture from the binary mixture of cationic and anionic dyes that suitably mimics real world wastewaters containing variety of industrial effluents.[44] To further improve the mechanical strength of the beads and enhance their stability against harsh acidic conditions, the free amino groups of CS were made to react with the carbonyl group of GL, resulting in a stable imine linkage formation leading to the formation of a crosslinked network.[34] While crosslinking enhanced the durability of the beads, it reduced the swelling capacity of the beads, resulting in a more compact matrix with controlled pore sizes, which is optimal for the adsorption of dyes.[35]Beads with elevated GL concentration exhibited better adsorption capacity, which may be attributed to the greater crosslink density imparted by the increased glutaraldehyde concentration, which resulted in better dye uptake as the more densely crosslinked CS network maintained a robust and stable architecture, effectively controlling excessive swelling upon contact with aqueous solutions. This stabilises internal pore structure and preserves the porous network, enabling extensive access of the dye molecules to the available binding sites on the beads. However, GL concentration beyond 15mmol was avoided as the slurry became too viscous and bead formation became unfeasible. To further enhance

adsorption capacity and surface functionality, grafting of HEMA onto the beads via KPS-initiated free-radical polymerisation was made, which introduced additional hydroxyl groups, improving hydrophilicity and facilitating hydrogen bonding interaction with the dye molecules. Adsorption experiments with CSK 7 beads were performed, but did not show any significant dye removal. Thus, the incorporation of HEMA as grafting monomer was essential. Optimal grafting was attained at 0.57mmol HEMA, balancing swelling capacity and crosslink density without inducing homopolymerisation or polymer matrix densification. Grafting was not carried out on the bead surface over 1.71mmol HEMA because homopolymer formed instead of grafting on CS-kaolin beads as a whitish, rubbery, or gel-like substance. The polymer matrix became extremely dense, and there were more opportunities for homopolymerisation rather than grafting in the case of beads containing 1.14mmol or 1.71mmol HEMA. Better yield was observed with CSK 4 than CSK 6, as the latter had higher kaolin content, which led to leaching of kaolin from the surface of the beads due to poor CS-kao binding during mechanical stirring. Due to the higher quantity of kaolin in CSK 6 beads, an unequal balance between the kaolin particles and chitosan matrix took place and caused poor binding between kaolin and chitosan, which led to fragile bead formation and leaching of the surplus kaolin particles. Thus, CS:Kao beyond 1:2 was not made, and CSK 4 variant was found to be most effective with an optimal balance between organic and inorganic counterparts along with crosslinker density. There is a possibility of n-π interaction between the lone pair of electrons on the oxygen atom of the hydroxyl group and the aromatic ring present in the molecular structure of CV dye[37] and π- π stacking interaction between the aromatic rings of CR and CV dyes in the binary mixture (Fig. 2). The presence of hydroxyl groups of Kao, along with HEMA, also offers hydrogen bonding interaction with the electronegative O and N atoms present in the dyes.[36]Another type of hydrogen bonding interaction known as Yoshida H-bonding between -OH groups on the surface of the beads and the CV ring could play a crucial role in the adsorption of cationic CV dye under acidic pH conditions. [37, 38]

3.2 FTIR Spectroscopy:

The infrared spectra of neat CSK 4 beads and AC-20 beads before and after dye adsorption are shown in Fig. 1. The main characteristic peaks in neat CS: the broad peak at 3430 cm^{-1} was attributed to the overlapping between O-H and N-H bond stretching frequencies[39] which were hydrogen bonded leading to their broadening and the band at 2914 cm^{-1} indicated aliphatic C-H stretching vibrations[39] present in the polysaccharide chains of CS, peak at 1456 cm^{-1} was assigned as C-H bending vibrations[40] and it was retained in all the IR spectrums with slight shifting, the strong band at 1029 cm^{-1} was due to C-O-C stretching vibrations[41] which highlighted the glycosidic linkage present in CS biopolymer. The CSK 4 peaks showed a band at 3448 $cm^{-1,}$ which was attributed to the overlapping O-H and N-H bond stretching frequencies as present in CS as well as Kaolin. The new peak at 1662 cm^{-1} was of C = N stretching frequency[42] that indicated successful cross-linking by GL, which resulted in imine linkage formation, and it reduced after grafting of HEMA monomer, probably due to overlapping with the C = O peak of HEMA. The peak at 2914–2943 cm^{-1} region, which corresponds to aliphatic C-H stretching as

present in neat CS, AC-20 beads, both before and after dye adsorption, was found to be diminished or absent in the IR spectrum of CSK-4, which may be due to some sort of masking effect or peak broadening leading to overlapping with the O-H and N-H peaks. The appearance of a peak at 1705cm^{-1} in the IR spectrum of AC-20 was attributed to the C = O group[43], which proved successful grafting of HEMA monomer. HEMA grafting likely increased the overall aliphatic content, which enhanced the intensity of C-H stretching and led to reappearance of the peak near 2938 cm^{-1}. The peak around 1556 cm^{-1} corresponded to N-H bending vibration.[45] The band near 1062-1068cm^{-1} in the FTIR spectra of CSK-4 and AC-20 after incorporation of kaolin could be related to the stretching vibration of Si–O–Si and O–Si–O present in kaolin.[46] The peak at 1062 cm^{-1} is also attributed to the S = O peak of CR after dye adsorption, but as it overlapped with the Si-O-Si band of kaolin, it could not be distinctly identified.[47] The N = N peak of CR appears near 1446 $cm^{-1,}$ which was not prominently visible due to peak overlapping with the C-H bending vibrations.[47] In the IR spectrum of neat CS, a single peak at 1029 cm^{-1} corresponding to C-N bending was present, but it resembled a doublet type of appearance after incorporation of kaolin. The extra peak that appeared near 1004–1019 cm^{-1} could be assigned to the stretching vibration of the Si–O groups present in Kaolin. The distinct peaks around 515–786 cm^{-1} are attributed to Al–O–Si and Si–O–Si bending vibration.[15] After adsorption of dyes from the binary mixture, the intensity of O-H stretching frequency shows a sharp decrease which indicated the involvement of the hydroxyl groups of kaolin that were accumulated on the surface of the beads as evident from the SEM images (Fig. 4), as well as HEMA, in hydrogen bonding type interaction with the dye molecules The intensity of peaks near 1062-1068cm^{-1} decreased sharply after dye adsorption indicating the involvement of siloxane groups in hydrophobic interaction with the aromatic ring of CV molecules.[46]

3.3 Changes in Zeta Potential of the beads before and after adsorption:

The surface charge of the adsorbent beads before and post dye adsorption is listed in Table 3. Prior to adsorption, under neutral conditions, the surface charge of AC-20 beads was − 24.8 mV. However, after the adsorption of CR and CV dyes from their binary mixture at pH = 1, the surface charge increased to 36.4 mV. In contrast, after the adsorption of anionic CR dye alone at pH = 1, resulted in a surface charge of 1.47 mV only. This demonstrated that the adsorbent's surface was highly protonated, and a high positive charge was generated on the surface under acidic conditions. The relatively low positive surface charge after adsorption of CR alone can be attributed to the ability of the anionic dye to partially neutralise the protonated surface upon adsorption. However, in the binary dye mixture, the surface charge substantially increased to 36.4mV, reflecting the successful adsorption of both cationic CV and anionic CR dyes. Such a strong positive shift of the surface charge was caused by both the protonated surface of the beads and the cationic CV dye. Despite the presence of anionic CR, this large positive shift showed that the cationic CV dye had strong affinity towards adsorption on the surface of the dye and

had accumulated on the surface due to strong non covalent interactions between the aromatic rings of the CV dye molecules and the hydroxyl groups present in the polymeric bead matrix where kao was accumulated on the outer surface as observed from the SEM images.[4]

Table 3
Zeta potential of adsorbent beads before and after adsorption for both stepwise and simultaneous adsorption:

Sample	**AC-20 (before adsorption)**	**AC-20 (after CR adsorption at pH = 1)**	**AC-20 (after CR and CV adsorption from their binary mixture at pH = 1)**	**AC-20 (CR followed by CV adsorption at pH = 1)**	**AC-20 (CV followed by CR adsorption at pH = 1)**	**AC-13 (after CR and CV adsorption from their binary mixture at pH = 11)**
Zeta Potential (mV)	-24.8	1.47	36.4	17.6	37.8	-15.2

3.4 Adsorption Mechanism:

It was observed that CR was successfully adsorbed by practically all the adsorbents under acidic pH, which was consistent with its anionic nature. At acidic pH, the surface of the adsorbent became protonated and thus the positively charged adsorbent surface provided a strong electrostatic interaction with the negatively charged CR molecules and facilitated with their rapid uptake which was demonstrated with the low positive shift of surface charge (Table 3) after adsorption of CR alone.[49] Thus, surface charge played a central role in controlling the uptake of anionic CR dye. In the absence of anionic CR dye, the removal efficiency of CV dye alone was sufficiently low, as visible from the UV plots. The strong electrostatic repulsion between the positively charged adsorbent surface and cationic dye moieties outweighed the non-covalent interactions, and thus, CV dye could not be adsorbed alone. Whereas, in the binary mixture of CR and CV, sufficient adsorption of CV was observed along with CR. This proved that the adsorption of CR assisted in the adsorption of CV, as in the absence of the former, the latter was not adsorbed by the adsorbent surface at all. Thus, upon adsorption of anionic dye, the surface of the adsorbent underwent modification, and the net positive charge of the surface diminished, which was also in agreement with zeta potential values. This exposed additional hydroxyl groups along with siloxane linkages on the bead's surface, which facilitated subsequent adsorption of cationic CV dye from their binary mixture. There was considerable interaction between the cationic and anionic dyes in their binary mixture, as observed from the shift in λ_{max} values from the original values of the individual dyes, and thus adsorption of one dye facilitated the entry of the other dye as well. This bathochromic shift of wavelength in the UV plot post adsorption was may be due to π-π stacking type interaction between the two dyes.[59] Thus, a cooperative type of binding took place where the presence of one dye

enhanced the adsorption of the other dye and increased the adsorption capacity. The siloxane sheets in kao provided a planar electron-rich surface, which likely facilitated hydrogen bonding, and the electron-rich layered arrangement behaved similar to π electron density of an aromatic ring and may have resulted in stacking-type interaction with the aromatic rings of CV dye. The aluminosilicate layers of kao had a planar sheet-like structure, which enhanced the effective surface area for adsorption and also provided numerous accessible adsorption sites. The layered structure of kao further aided in aligning the aromatic dye molecules for efficient packing that maximised the stacking type of interaction.[44] Kao along with HEMA, also provided a hydrophilic character that facilitated better dye diffusion. The adsorption mechanism of the binary dye systems was conclusively determined to be sequential and not concurrent as evidenced by zeta potential measurement. Adsorbent beads were made to adsorb CV followed by CR adsorption under an acidic environment and zeta potential value was found to be 37.8mV (Table 3) whereas adsorbent beads which adsorbed CR followed by CV adsorption showed a relatively lower surface charge of 17.6 mV (Table 3), suggesting that all the available adsorbent sites were already saturated by CR under acidic pH so very few adsorbent sites were available for adsorption of CV. The zeta potential of the beads after exposure to a binary mixture of CV and CR dyes was found to be 36.4 mV, which closely aligned with the surface charge of CV pre-adsorbed beads following CR uptake. This proved that sequential adsorption of one dye altered the physicochemical properties of the adsorbent beads and influenced the dye adsorption dynamics. CV being smaller in size and more compact as compared to CR, where the two naphthalene rings created substantial bulkiness and thus, in a binary mixture, it probably led to faster adsorption of smaller CV molecules due to steric reasons. The adsorption of CV on the adsorbent surface was done by hydrogen bonding[15] and stacking interaction, so it was accumulated on the surface as observed in the SEM images and played a dominating role in surface charge determination. In the binary dye mixture, the attraction between anionic CR and cationic CV due to opposite charges, along with π-π stacking type of interaction between the aromatic rings of the dye molecules, could also favour synergistic adsorption of CV, which could not be adsorbed in the absence of CR.[50] The adsorption mechanisms are shown in Fig. 2.

3.5 Variation of Swelling:

The swelling behaviour of the beads with reference to a specific time frame reflects a plot which is influenced by both inorganic kao acting as filler and HEMA acting as grafting agent. Upon immersion in water, the polymer beads exhibited an initial increase in swelling capacity followed by a distinct decline in swelling due to the rearrangement of polymer chains before reaching equilibrium. With an increase in the amount of crosslinker (GL), swelling capacity was found to decrease as the polymer network became denser and thus a lower number of available sites were available for water absorption, leading to lower swelling.[35]

Beads without kao (AC-1) exhibit a substantially high swelling capacity as the inorganic kao particles acted as fillers and offered resistance to penetration of water into the beads and enhanced the rigidity of the beads. The absence of fillers facilitated water diffusion to a large extent. The mechanical stiffness

introduced by kao to the beads limited the chain mobility and thus suppressed the swelling capacity and thus with an increase in the inorganic clay content, the beads exhibited a relatively lower swelling. With the introduction of HEMA, the hydrophilicity of the network was enhanced, which led to an increase in swelling capacity. Thus, with an increase in the concentration of grafting monomer, water absorption capacity increased and showed higher swelling.[51] The variation of maximum swelling capacity by various variants, which included different kao content, GL and HEMA concentration, is represented in the form of a bar graph (Fig. 3).

3.6 Morphological and elemental analysis of the beads before and post dye adsorption:

Macroscopic investigation was done after bead formation, and pictures were captured after drying the beads using a portable camera. (Fig. 2a) Beads were observed to be yellowish-white in colour, mostly uniform in shape and spherical. Upon drying, the beads underwent shrinkage due to loss of water by air-drying, and the surface became rough and leading to the formation of irregular cracks. Surface morphology and characteristics of the adsorbents were investigated by Scanning Electron Microscopy. The surface had a structure with irregular cavities. It had numerous cracks or crinkles along with a rough, heterogeneous surface. Thus, the SEM images of the beads before adsorption demonstrated that they were a potential adsorbent, as they had numerous sites for dye diffusion. The SEM images of beads (Fig. 4) having higher kao content (CSK 6) had aggregation of clay particles on the surface and led to a relatively more granular and crustier surface with increased roughness.[15]The difference in surface morphology of the beads with variation in kao content indicated the aggregation of inorganic clay particles on the surface of the beads which could thus influence the adsorption of cationic CV dye from the binary dye mixture under acidic pH greatly, where electrostatic interactions could not be the sole reason of adsorption and thus increasing the role of strong non-covalent interactions between the dye and bead's surface, which could be possible only if kao was accumulated on the surface. The surface morphology of the beads after dye adsorption underwent a change. After exposure to the binary dye mixture, the surface became relatively smoother due to the filling up of the pores by the CR and CV dye molecules.[52] The surface of the beads was relatively less textured and more homogenous as the dye molecule coated and adhered to the bead surface and leading to decreased roughness. The presence of silicon and aluminium (Si = 0.69%, Al = 0.54%) (Figure S6) was revealed by the elemental analysis of the AC-20 beads, which in turn demonstrated the existence of aluminosilicate sheets in kao. But, kao contained other impurities like potassium and sodium due to the presence of K_2O and Na_2O which was observed from EDX data (Na = 0.5, K = 0.14).[53]Elemental analysis of the beads after dye adsorption (Figure S6) revealed the presence of chlorine (Cl) and sulfur (S), which indicated that the CV and CR dyes had been successfully adsorbed from their binary mixture.

3.7 XRD Analysis:

The XRD patterns of CSK4, CSK7 and AC-20 beads are illustrated in Fig. 5. The preservation of the kaolin clay structure in the polymer matrix was confirmed by prominent diffraction peaks near 2θ = 26.9°, 34.1° and 37.2° in CSK-4 and AC-20.[15] The sharp peak indicated that the ordered silicate layers were retained even after polymer incorporation. The semi-crystalline structure of chitosan is apparent by a broad, intense diffraction peak in AC-20 between 2θ = 19.4° and 21.6°.[62] The incorporation of hydrophilic HEMA promotes extensive hydrogen-bonded segments, which facilitates structural ordering and crystal alignment, which provided highest crystallinity percentage of 79.3% to AC-20. Strong direct hydrogen bonding between the hydroxyl and amino groups of chitosan and the hydroxyl groups of kaolin occurred in CSK-4, resulting in a more rigid and compact structure, but the hindered chain rearrangement decreased the crystallinity to 71.1%. Despite the lack of inorganic clay, CSK-7 showed 49.5% crystallinity, which was direct evidence of structural reorganisation brought by covalent crosslinking. The main crystal size was 22.2 nm at the maximum intensity peak around 29.3° for AC-20 which was calculated according to the reported Debye Scherer's equation.[15]

3.8 Effect of pH on dye removal from binary mixture:

The UV-Vis spectra of the binary dye mixtures did not display any distinct absorption peaks for individual dyes present in the binary mixture, likely due to significant spectral overlap, which led to peak broadening. For identification and quantification of the individual dye peaks, deconvolution[54]was done using Origin Pro software and the absorbance values of both the peaks were recorded, which were subsequently used to determine the concentration of each dye remaining in the solution after adsorption from the calibration curves. The adsorption behaviour of the composite beads was highly pH dependent, governed by its surface charge, ionisation of the functional groups present in the adsorbent beads and the interplay between dye-adsorbent and dye-dye interactions. The effect of pH on dye removal was experimentally evaluated under a pH range from 1 to 11 (Fig. 6), initial concentration of dyes was 10 mg/L and an adsorbent dosage of 0.05 g was uniformly maintained, and all experiments were performed at room temperature.

Under an acidic environment, AC-20 beads demonstrated a maximum removal efficiency achieving up to 99.7% for CR and 95.4% for CV at pH = 1 (Figure S3, showing the deconvoluted UV plot). Under high acidic environment, the amino groups underwent protonation, resulting in high density of positively charged adsorption sites which was evidenced by a significant positive shift in zeta potential value as well, thereby fostering strong electrostatic attraction towards anionic CR dye.[52] Such pH dependent behaviour, using such low pH for extensive dye binding was observed in [48] where positively charged adsorbent surface was used for removal of anionic dye from the system. Adsorption of cationic CV dye was also enhanced under a strongly acidic environment, but this was solely dependent on the presence of CR in the binary mixture. The cooperative effect caused by CR dye molecules was significant, as in the absence of CR, CV remained completely unabsorbed as observed from the UV plots, which was obvious due to electrostatic repulsion and competitive adsorption of the H^+ ions, which were present in high concentration under the acidic pH of 1 instead of cationic CV moieties. In a binary mixture, the presence

of CR enhanced the adsorption of CV by altering the local microenvironment of the adsorbent and the attractive interaction between the cationic and anionic dyes present in the binary mixture also led to better dye binding. Although the maximum adsorption was achieved at pH 1, the beads retained high removal efficiencies of 84.9% for Congo Red and 91.9% for Crystal Violet at pH 3. This indicates that efficient co-adsorption is maintained throughout the acidic pH range, although the extent of protonation decreases with increasing pH. The acidic pH also enabled secondary interactions like strong hydrogen bonding type interactions and hydrophobic interactions between the Si-O-Si linkage of siloxane groups present in the kao groups and the aromatic CV molecules, as observed in the lowering of peak intensity of Si-O stretching in the FTIR spectrum post dye adsorption, which further promoted the adsorption of cationic CV dye. Thus, both cationic and anionic dyes were adsorbed from their binary mixture and this synergistic effect observed in dye removal demonstrated the effectiveness of our developed adsorbent for the treatment of real-world wastewater containing multiple dye pollutants obtained from textile industries. As pH increases from 1 to 7, the removal of dyes dropped significantly, being lowest at pH = 7. The removal efficiency towards cationic CV was a bit higher than that of anionic CR at pH = 7, as expected from the zeta potential value of AC-20 surface, which was negatively charged and thus had better affinity towards cationic CV dye molecules. With an increase in pH, the availability of protonated surface diminished, and thus, electrostatic attraction towards anionic CR was less prominent. As the adsorption of CR decreased, the surface charge could not be neutralised well, and it led to a cooperative decrease in the adsorption of CV. With an increase in pH, the possibility of hydrogen bonding also reduced as it gradually led to deprotonation of the hydroxyl units. These observations suggest that hydrogen bonding may contribute to the adsorption process together along with electrostatic interactions. As pH increased from pH = 7 to 11, removal efficiency further increased, but at pH = 11, only 57.5% CR removal and 21.8% CV removal from their binary mixture was observed by the AC-20 sample. At basic or neutral pH, protonation of the adsorbent surface was not possible, so adsorption of anionic CR by electrostatic attraction was not facilitated. The coexistence of CR in the binary mixture altered the surface environment, and it may also cause dye-dye interaction, leading to aggregation of both dyes in solution, which affected the adsorption of individual CV dye despite it being cationic under basic pH. The size of CV molecules was much larger than compared to linear CR molecules due to the presence of bulky aromatic rings, so the adsorption of CV molecules was sterically inhibited. Deprotonation of the hydroxyl groups at basic pH also diminishes the hydrogen bonding possibility which may be another reason for adsorption not being that effective at basic pH. Whereas, AC-13 variant demonstrated 91.5% CR removal and 80.2% CV removal. This was also supported by the zeta potential value of AC-13 beads post-dye adsorption, which indicated a surface charge of -15.2 mV (Table 3).The positive shift of surface charge from − 24.8mV to -15.2mV was not that high, since the medium being highly basic, the surface of the adsorbents would be negatively charged due to the presence of multiple deprotonated hydroxyl units and thus prone to adsorption of cationic dye, so a much higher positive shift of surface charge was expected but this minimal increase in zeta value clearly indicated both cationic and anionic dyes had been successfully adsorbed. This may be due to a more hydrophilic network in AC-13 (higher HEMA content) which allowed improved swelling and thus facilitated better penetration and diffusion of dye. Thus, with variation of HEMA content, the adsorption behaviour was significantly modified, which further

supports the reason behind using HEMA as the grafting monomer. Thus, the developed beads explored a unique blend where each component plays a special role in multi-dye adsorption models, and their variation leads to a completely new dye adsorption dynamic. The interplay between layered hydrophobic siloxane units of the surface embedded kao, along with the presence of hydrophilic hydroxyl groups of kao and HEMA, with variation of pH, was able to demonstrate efficient co-removal of noxious cationic and anionic dyes present together in their binary mixture.

3.9 Effect of adsorbent dosage on dye removal from binary mixture:

Different amounts of adsorbent beads (0.0125 g to 0.1 g) were used for the adsorption of 10 ppm solution of a binary mixture of CR and CV dyes at 40°C for 240 min at pH 1 (Fig. 6). With an increase in adsorbent dosage, till 0.025g dye removal percentage increased significantly, which may be attributed to the increase in the number of available adsorption sites for the removal of CR and CV dyes from their binary mixture. Almost complete removal of CR (99.7% removal) and CV (95.4%) was observed with 0.025 g AC-20 adsorbent beads, therefore, further increase in adsorbent dosage did not increase dye removal efficiency, rather it decreased considerably for CR and remained almost constant for CV, which may be due to saturation of all the available adsorption sites owing to efficient dye binding. Although there was a problem of leaching of kao particles from the surface while grafting of monomer in AC-22, but it showed excellent dye removal, leading to 99.7% removal of CR and 99.8% removal of CV when 0.1g of adsorbent beads were used. The increase in removal efficiency was due to the higher kao content of AC-22 beads which provided better non-covalent bindings with CV molecules.[55]

3.10. Adsorption Kinetics Studies:

In order to investigate the kinetics and adsorption mechanisms of the CR and CV dyes on the hybrid beads, a detailed kinetics study was conducted and the amount of adsorbent at equilibrium, q_e(mg/g) was estimated from the curve of q_t vs. t and compared with the value of q_e calculated from the best-fitted curves. The equilibrium time between adsorbate and adsorbent was investigated at an initial dye concentration of 10 mg/L in the range of (1-240) min. The best performing sample AC-20, which demonstrated the highest adsorption ability for both dyes, was selected for kinetics studies. It was observed that dye removal enhanced with time and reached equilibrium after 240 minutes, which indicated that a large number of active sites were available on the surface of the adsorbent in earlier stages for dye adsorption. Over time, the active sites became saturated and thus the rate of adsorption gradually slowed down and reached equilibrium after 240 minutes. Several kinetic models were employed, including pseudo-first order, pseudo-second order, second order and intraparticle diffusion models to assess time-based adsorption dynamics and equilibrium behaviour of both CR and CV dyes. The linear forms of these kinetic models are represented in equations (4) to (7):[56]

Pseudo First order: A plot of log(q_e-q_t) vs. t was made, where k_1 is the rate constant of the pseudo first order kinetics model.

$$log(q_e - q_t) = log\, q_e - \frac{k_1 t}{2.303}$$ -------(4)

Second order: A plot of 1/(q_e–q_t) vs. t was made, and k_s is the rate constant of the second-order kinetics model.

$$\frac{1}{q_e - q_t} = \frac{1}{q_e} + k_s t$$ -------(5)

Pseudo Second order: A plot of t/q_t vs. t was made and k_2 is the rate constant of the pseudo-second order kinetics model.

$$\frac{t}{q_t} = \frac{1}{k_2 q_e^2} + \frac{t}{q_e}$$ -------(6)

Intraparticle diffusion: A plot of q_t vs. $t^{1/2}$ was made and k_i denotes the rate constant.

$q_t = k_i\, t^{1/2} + 1$ -------(7)

The kinetics model fitting plots for pseudo-first order, second order, pseudo-second order and intraparticle diffusion for CR and CV dyes are shown in Figures S4 and S5. From various Kinetics Model fitting, it was observed that both CR and CV adsorption followed the pseudo-second order model (R^2 value was closest to 1) (Table ST1) and closer agreement between calculated and observed adsorption capacities. Thus, chemisorption may govern the adsorption process.[57] The value of qe (calculated) was obtained from the slope of the curve (Eq. 3) and q_e (experimental) were represented in Table ST1.

3.11. Desorption:

A series of solvents was used, including HCl, NaOH, hot water and 70% ethanol for performing desorption experiments in order to evaluate and prove the nature of dye interactions with the surface of the beads. Among these, the most effective reagent for desorption of both dyes was found to be 70% ethanol. [58] The superior desorption efficiency of a polar protic solvent, ethanol, further suggested that non-covalent interactions played a significant role in the adsorption process, and they could be disrupted by ethanol, leading to their effective release effectively. Reagents like HCl, NaOH primarily modulate the electrostatic attractions between the adsorbate surface and dye molecules and their ineffectiveness towards desorption clearly depicted that the adsorption process was not merely influenced by ionic interactions. Thus, the developed adsorbent beads showed a unique behaviour of removing both cationic and anionic dyes via co-adsorption at the same pH.

Conclusion

Most of the studies found in the literature (reported in Table 4) were targeted to remove a single dye alone at a certain specific pH condition. From the present study, it can be concluded that, among the various variants of organic-inorganic hyphenated beads that were synthesised, the most promising candidates for dual dye removal having diverse character were AC-20 beads, where an optimum balance between the organic and inorganic counterparts was present with an efficient crosslinked network and hydrophilicity.AC-22 beads also showed significant dye removal capacities, leading to 99.7% CR removal and 99.8% CV removal, but the adsorbent dosage was higher as compared to AC-20 and there was also a problem of leaching of inorganic clay particles. FTIR spectra XRD and SEM images were direct evidence of successful incorporation of inorganic clay on the outer surface of polysaccharide backbone, crosslinking resulting in imine linkage formation, grafting on the surface of beads and morphological changes on the surface of the beads post dye binding. Anionic CR showed 99.7% removal and cationic CV exhibited 95.4% removal by AC-20 sample. Most of the previous studies were concerned with single dye removal at a time. The novelty of our work lies in the co-adsorption of anionic and cationic dyes from their binary mixture at same pH by using hyphenated beads as adsorbents. The synthesised beads have the potential to be used universally for various other cationic and anionic dyes present in significant amounts and is a threat towards the environment. This is mainly attributed to their unique structural feature, which enabled various types of interactions, including electrostatic and non-covalent type interactions, facilitating broad-spectrum dye removal in the field of wastewater treatment. Thus, AC-20 beads and related formulations could be used as a promising candidate for designing a fixed-bed column that would enable continuous removal of wastewater containing binary dye mixtures, which would also be highly beneficial from an industrial point of view.

Table 4
Comparison of the removal capacity of CV and CR dyes with related data available in the literature

Adsorbent	Dye removed	Removal %	Reference	Operational pH	Time taken for removal	Single/Binary
AC-20	CR	99.7	Present work	1	240 mins	Binary
AC-20	CV	95.4	Present work	1	240 mins	Binary
AC-22	CR	99.7	Present work	1	240 mins	Binary
AC-22	CV	99.8	Present work	1	240 mins	Binary
Raw Chitin	CR	82.15	61	2	45 mins	Single
Raw Chitin	CV	99.47	61	12	45 mins	Single
Brazilian palygorskite	CR*	98	22	Basic pH	240 mins	Single (at a time)
Brazilian palygorskite	CV*	98	22	Basic pH	240 mins	Single (at a time)
Kaolin impregnated aminated chitosan beads	CR	90.7	25	6	45 mins	Single
Chitosan beads	CV	90	60	10	90 mins	Single

*not clearly mentioned whether both cationic and anionic dyes were taken together or separately treated.

Declarations

Ethical Statement:

No approval was required.

Funding Statement:

There is no funding interest related to this research work.

Author Contribution

i. Arundhati Chakraborty: Conceptualization, Data curation, Formal analysis, Investigation, Methodology, Validation, Visualization, Writing-original draft, Writing-review and editingii. Sonai Dutta: Formal analysis, Methodology, Visualizationiii. Reetika Sarkar: Formal analysis, Visualizationiv. Debasis Brahma: Formal analysis, Visualizationv. Anirban Mukherjee: Data curation, Resourcesvi. Amit Sen: Data curation, Resourcesvii. Prasenjit Ghosh: Data curation, Resourcesviii. Rabindra Mukhopadhyay: Data curation, Resourcesix. Suman Acharya: Data curation, Resourcesx. Debdipta Basu: Data curation, Resourcesxi. Arjun Maity: Writing-review and editingxii. Abhijit Bandyopadhyay: Conceptualization, Formal analysis, Investigation, Methodology, Supervision, Validation, Visualization, Writing-review and editing

References

1. Dutta S, Gupta B, Srivastava SK, Gupta AK (2021) Recent advances on the removal of dyes from wastewater using various adsorbents: a critical review. Mater Adv 2(14):4497–4531. https://doi.org/10.1039/d1ma00354b
2. Thottathil S, Puttaiahgowda YM, Selvaraj R, Elambalassery JG, Vinayagam R, Varadavenkatesan T (2025) Experimental and DFT studies of Congo red and AB 113 dyes removal by adsorption and disinfection using novel triazine-based porous organic polymer. J Mol Liq 127628. https://doi.org/10.1016/j.molliq.2025.127628
3. Islam A, Teo SH, Taufiq-Yap YH, Ng CH, Vo DN, Ibrahim ML, Hasan MM, Khan MaR, Nur AS, Awual MR (2021) Step towards the sustainable toxic dyes removal and recycling from aqueous solution- A comprehensive review. Resour Conserv Recycling 175:105849. https://doi.org/10.1016/j.resconrec.2021.105849
4. Slama HB, Bouket AC, Pourhassan Z, Alenezi FN, Silini A, Cherif-Silini H, Oszako T, Luptakova L, Golińska P, Belbahri L (2021) Diversity of Synthetic Dyes from Textile Industries, Discharge Impacts and Treatment Methods. Appl Sci 11(14):6255. https://doi.org/10.3390/app11146255
5. Haleem A, Shafiq A, Chen S, Nazar M (2023) A Comprehensive Review on Adsorption, Photocatalytic and Chemical Degradation of Dyes and Nitro-Compounds over Different Kinds of Porous and Composite Materials. Molecules 28(3):1081. https://doi.org/10.3390/molecules28031081
6. Iqbal J, Shah NS, Sayed M, Niazi NK, Imran M, Khan JA, Khan ZUH, Hussien AGS, Polychronopoulou K, Howari F (2020) Nano-zerovalent manganese/biochar composite for the adsorptive and oxidative removal of Congo-red dye from aqueous solutions. J Hazard Mater 403:123854. https://doi.org/10.1016/j.jhazmat.2020.123854
7. Mirza A, Ahmad R (2020) An efficient sequestration of toxic crystal violet dye from aqueous solution by Alginate/Pectin nanocomposite: A novel and ecofriendly adsorbent. Groundw Sustainable Dev 11:100373. https://doi.org/10.1016/j.gsd.2020.100373
8. Saeed A, Sharif M, Iqbal M (2010) Application potential of grapefruit peel as dye sorbent: Kinetics, equilibrium and mechanism of crystal violet adsorption. J Hazard Mater 179(1–3):564–572. https://doi.org/10.1016/j.jhazmat.2010.03.041

9. Ding J, Zhang Q, Zeng Z, Zhao Z, Zhang Y, Wang F, Tian D, Zhang S (2025) Enhanced removal of tetracycline using UiO-66-NH2/modified chitosan composite adsorbent. Mater Sci Eng B 323:118736. https://doi.org/10.1016/j.mseb.2025.118736
10. Qian L, Zhao Q, Lin Y, Yang J, Qin Z (2026) Lignin@Polypyrrole nanoparticles Enhanced hydrogel for recyclable Congo Red dye adsorption. J Appl Polym Sci. https://doi.org/10.1002/app.70580
11. Bhatt P, Joshi S, Bayram GMU, Khati P, Simsek H (2023) Developments and application of chitosan-based adsorbents for wastewater treatments. Environ Res 226:115530. https://doi.org/10.1016/j.envres.2023.115530
12. Shen C, Shen Y, Wen Y, Wang H, Liu W (2011) Fast and highly efficient removal of dyes under alkaline conditions using magnetic chitosan-Fe(III) hydrogel. Water Res 45(16):5200–5210. https://doi.org/10.1016/j.watres.2011.07.018
13. Sheraz M, Sun X, Siddiqui A, Hu S, Song Z (2025) Research advances in natural polymers for environmental remediation. Polymers 17(5):559. https://doi.org/10.3390/polym17050559
14. Shen C, Song S, Zang L, Kang X, Wen Y, Liu W, Fu L, Shen C, Song S, Zang L, Kang X, Wen Y, Liu W, Fu L (2009) Efficient removal of dyes in water using chitosan microsphere supported cobalt (II) tetrasulfophthalocyanine with H2O2. J Hazard Mater 177(1–3):560–566. https://doi.org/10.1016/j.jhazmat.2009.12.069
15. Alsoaud MMA, Taher MA, Hamed AM, Elnouby MS, Omer AM (2022) Reusable kaolin impregnated aminated chitosan composite beads for efficient removal of Congo red dye: isotherms, kinetics and thermodynamics studies. Sci Rep 12(1). https://doi.org/10.1038/s41598-022-17305-w
16. Varshan GA, Namasivayam SKR, Sowmya R, Sivasuriyan KS (2025) Design and optimization of a bio-nano adsorption batch system using fungal-based chitosan nanoparticles for crystal violet removal from aqueous media. J Water Process Eng 81:109342. https://doi.org/10.1016/j.jwpe.2025.109342
17. Miao L, Hu L, Mao X, Yang R, Hong Z, Zhao J, Chen J, Huang S, Tan J, Chen Y, Wang Y, Qian Z, Zhu Z (2025) Epichlorohydrin cross-linked chitosan for adsorption of reactive red 2 dye: Optimization and adsorption mechanism. Int J Biol Macromol 320:146202. https://doi.org/10.1016/j.ijbiomac.2025.146202
18. Cagnetta G, Yin Z, Qiu W, Vakili M (2024) Mechanochemical Synthesis of Cross-Linked Chitosan and Its Application as Adsorbent for Removal of Per- and Polyfluoroalkyl Substances from Simulated Electroplating Wastewater. Materials 17(12):3006. https://doi.org/10.3390/ma17123006
19. Lavlinskaya MS, Sorokin AV, Mikhaylova AA, Kuznetsov EI, Baidamshina DR, Saranov IA, Grechkina MV, Holyavka MG, Zuev YF, Kayumov AR, Artyukhov VG (2024) The Low-Waste grafting copolymerization modification of chitosan is a promising approach to obtaining materials for food applications. Polymers 16(11):1596. https://doi.org/10.3390/polym16111596
20. Wang P, Shen X, Qiu S, Zhang L, Ma Y, Liang J (2024) Clay-Based Materials for Heavy Metals Adsorption: Mechanisms, advancements, and future Prospects in environmental remediation. Crystals 14(12):1046. https://doi.org/10.3390/cryst14121046

21. Pereira FA, Sousa KS, Cavalcanti GR, França DB, Queiroga LN, Santos IM, Fonseca MG, Jaber M (2017) Green biosorbents based on chitosan-montmorillonite beads for anionic dye removal. J Environ Chem Eng 5(4):3309–3318. https://doi.org/10.1016/j.jece.2017.06.032
22. Silva VC, Araújo MEB, Rodrigues AM, Vitorino MDBC, Cartaxo JM, Menezes RR, Neves GA (2021) Adsorption behavior of Crystal violet and Congo red dyes on Heat-Treated Brazilian Palygorskite: Kinetic, Isothermal and Thermodynamic studies. Materials 14(19):5688. https://doi.org/10.3390/ma14195688
23. Fizir M, Touil S, Richa A, Wei L, Douadia S, Taibi R, Cherifi S, Mansuroglu DS, Dramou P (2024) Kaolin-iron cross-linked alginate beads for efficient phosphate removal from water: An initiation towards sustainable treatment of domestic and hydroponic wastewaters. Appl Clay Sci 256:107430. https://doi.org/10.1016/j.clay.2024.107430
24. Biswas S, Rashid TU, Debnath T, Haque P, Rahman MM (2020) Application of Chitosan-Clay Biocomposite Beads for Removal of Heavy Metal and Dye from Industrial Effluent. J Compos Sci 4(1):16. https://doi.org/10.3390/jcs4010016
25. Negrea A, Mihailescu M, Mosoarca G, Ciopec M, Duteanu N, Negrea P, Minzatu V (2020) Estimation on Fixed-Bed Column Parameters of Breakthrough Behaviors for Gold Recovery by Adsorption onto Modified/Functionalized Amberlite XAD7. Int J Environ Res Public Health 17(18):6868. https://doi.org/10.3390/ijerph17186868
26. Joseph J, Väisänen A, Patil AB, Lahtinen M (2023) The effect of synthesis conditions on the in situ grown MIL-100(Fe)-chitosan beads: Interplay between structural properties and arsenic adsorption. J Hazard Mater 463:132893. https://doi.org/10.1016/j.jhazmat.2023.132893
27. Öztürk S, Demir N (2023) Preparation of poly(2-hydroxyethyl methacrylate)-grafted chitosan-montmorillonite superabsorbent nanocomposite for adsorption of bovine serum albumin. Polym Adv Technol 34(10):3345–3355. https://doi.org/10.1002/pat.6148
28. Wekoye JN, Wanyonyi WC, Wangila PT, Tonui MK (2020) Kinetic and equilibrium studies of Congo red dye adsorption on cabbage waste powder. Environ Chem Ecotoxicol 2:24–31. https://doi.org/10.1016/j.enceco.2020.01.004
29. Pandey A, Bithel N, Kumar S, Kumar S (2025) A sustainable method of crystal violet dye removal using novel strain Klebsiella pneumoniae ED2. Sustainable Chem Environ 100210. https://doi.org/10.1016/j.scenv.2025.100210
30. Pal A, Majumder K, Sengupta S, Das T, Bandyopadhyay A (2017) Adsorption of soluble Pb(II) by a photocrosslinked polysaccharide hybrid: A swelling-adsorption correlation study. Carbohydr Polym 177:144–155. https://doi.org/10.1016/j.carbpol.2017.08.122
31. Dutta S, Basak S, Bandyopadhyay A (2025) Binary-Grafted Chitosan-Based hydroxyethyl methacrylate and glycidyl trimethylammonium chloride copolymers for selective removal of kaolin suspension and anionic dyes via flocculation. Polym Eng Sci. https://doi.org/10.1002/pen.70110
32. Aranaz I, Alcántara AR, Civera MC, Arias C, Elorza B, Caballero AH, Acosta N (2021) Chitosan: An overview of its properties and applications. Polymers 13(19):3256.

https://doi.org/10.3390/polym13193256

33. Han Y, Yan Z, Jin L, Liao J, Feng G (2020) In situ study on interactions between hydroxyl groups in kaolinite and re-adsorption water. RSC Adv 10(29):16949–16958. https://doi.org/10.1039/d0ra01905d
34. Barbosa RFS, Shyam S, Misra S, Mitra SK, Rosa DS (2025) Chitosan hydrogels crosslinked with glutaraldehyde for potential toxic elements removal: Batch and purification device analysis. J Appl Polym Sci. https://doi.org/10.1002/app.57539
35. Hoti G, Caldera F, Cecone C, Pedrazzo AR, Anceschi A, Appleton SL, Monfared YK, Trotta F (2021) Effect of the Cross-Linking density on the swelling and rheological behavior of Ester-Bridged B-Cyclodextrin nanosponges. Materials 14(3):478. https://doi.org/10.3390/ma14030478
36. Ahmad R, Ejaz MO (2023) Efficient adsorption of crystal violet (CV) dye onto benign chitosan-modified l-cysteine/bentonite (CS-Cys/Bent) bionanocomposite: Synthesis, characterization and experimental studies. Dyes Pigm 216:111305. https://doi.org/10.1016/j.dyepig.2023.111305
37. Mecheri R, Zobeidi A, Atia S, Nacer SN, Salih AaM, Benaissa M, Ghernaout D, Arni SA, Ghareba S, Elboughdiri N (2023) Modeling and Optimizing the Crystal Violet Dye Adsorption on Kaolinite Mixed with Cellulose Waste Red Bean Peels: Insights into the Kinetic, Isothermal, Thermodynamic, and Mechanistic Study. Materials 16(11):4082. https://doi.org/10.3390/ma16114082
38. Parker HL, Hunt AJ, Budarin VL, Shuttleworth PS, Miller KL, Clark JH (2012) The importance of being porous: polysaccharide-derived mesoporous materials for use in dye adsorption. RSC Adv 2(24):8992. https://doi.org/10.1039/c2ra21367b
39. Alyasi H, Mackey H, McKay G (2023) Adsorption of Methyl Orange from Water Using Chitosan Bead-like Materials. Molecules 28(18):6561. https://doi.org/10.3390/molecules28186561
40. Islam S, Arnold L, Padhye R (2015) Comparison and Characterisation of Regenerated Chitosan from 1-Butyl-3-methylimidazolium Chloride and Chitosan from Crab Shells. *BioMed Research International*, *2015*, 1–6. https://doi.org/10.1155/2015/874316
41. Tzaneva D, Simitchiev A, Petkova N, Nenov V, Stoyanova A, Denev P (2017) Synthesis of Carboxymethyl Chitosan and its Rheological Behaviour in Pharmaceutical and Cosmetic Emulsions. J Appl Pharm Sci. https://doi.org/10.7324/japs.2017.71010
42. Zhang Y, Wang Q, Yan K, Qi Y, Wang G, Cui Y (2016) Preparation, characterization, and evaluation of genipin crosslinked chitosan/gelatin three-dimensional scaffolds for liver tissue engineering applications. J Biomedical Mater Res Part A 104(8):1863–1870. https://doi.org/10.1002/jbm.a.35717
43. Islas L, Burillo G, Ortega A (2018) Graft Copolymerization of 2-Hydroxyethyl Methacrylate onto Chitosan Using Radiation Technique for Release of Diclofenac. Macromol Res 26(8):690–695. https://doi.org/10.1007/s13233-018-6100-6
44. Shahinpour A, Tanhaei B, Ayati A, Beiki H, Sillanpää M (2022) Binary dyes adsorption onto novel designed magnetic clay-biopolymer hydrogel involves characterization and adsorption performance:

Kinetic, equilibrium, thermodynamic, and adsorption mechanism. J Mol Liq 366:120303. https://doi.org/10.1016/j.molliq.2022.120303

45. Praxedes A, Webler G, Souza S, Ribeiro A, Fonseca E, De Oliveira I (2016) Non-monotonic wetting behavior of chitosan films induced by silver nanoparticles. Appl Surf Sci 370:25–31. https://doi.org/10.1016/j.apsusc.2016.01.264
46. Belkassa K, Khelifa M, Batonneau-Gener I, Marouf-Khelifa K, Khelifa A (2021) Understanding of the mechanism of crystal violet adsorption on modified halloysite: Hydrophobicity, performance, and interaction. J Hazard Mater 415:125656. https://doi.org/10.1016/j.jhazmat.2021.125656
47. Moon SA, Salunke BK, Saha P, Deshmukh AR, Kim BS (2018) Comparison of dye degradation potential of biosynthesized copper oxide, manganese dioxide, and silver nanoparticles using Kalopanax pictus plant extract. Korean J Chem Eng 35(3):702–708. https://doi.org/10.1007/s11814-017-0318-4
48. Qin Y, Wang L, Zhao C, Chen D, Ma Y, Yang W (2016) Ammonium-Functionalized hollow polymer particles as a PH-Responsive adsorbent for selective removal of acid dye. ACS Appl Mater Interfaces 8(26):16690–16698. https://doi.org/10.1021/acsami.6b04199
49. Bingöl MS (2024) Efficient removal of congo red and cytotoxicity evaluation of biosorbents prepared from chitosan-added watermelon pulp. Sci Rep 14(1). https://doi.org/10.1038/s41598-024-74010-6
50. Khomri ME, Messaoudi NE, Dbik A, Bentahar S, Lacherai A, Chegini ZG, Iqbal M (2021) Organic Dyes Adsorption on the Almond Shell (Prunus dulcis) as Agricultural Solid Waste from Aqueous Solution in Single and Binary Mixture Systems. Biointerface Res Appl Chem 12(2):2022–2040
51. Durmuş S, Yılmaz B, Onder A, Ilgin P, Ozay H, Ozay O (2022) An innovative approach to use zeolite as crosslinker for synthesis of p(HEMA-co-NIPAM) hydrogel. Monatshefte Für Chemie - Chem Monthly 153(4):369–382. https://doi.org/10.1007/s00706-022-02908-w
52. Litefti K, Freire MS, Stitou M, González-Álvarez J (2019) Adsorption of an anionic dye (Congo red) from aqueous solutions by pine bark. Sci Rep 9(1). https://doi.org/10.1038/s41598-019-53046-z
53. Dewi R, Agusnar H, Alfian Z, Tamrin N (2018) Characterization of technical kaolin using XRF, SEM, XRD, FTIR and its potentials as industrial raw materials. *Journal of Physics Conference Series*, *1116*, 042010. https://doi.org/10.1088/1742-6596/1116/4/042010
54. Ratnam D, Das SK, Jasuja K (2017) Ionic liquid assisted exfoliation of layered magnesium diboride. *IOP Conference Series Materials Science and Engineering*, *225*, 012111. https://doi.org/10.1088/1757-899x/225/1/012111
55. Chung W, Ong S (2021) Effective removal of Reactive Brown 10 from aqueous solution by using chitosan beads: Batch and experimental design studies. J Phys Sci 32(1):91–108. https://doi.org/10.21315/jps2021.32.1.7
56. Pal A, Giri A, Bandyopadhyay A (2016) Influence of hydrodynamic size and zeta potential of a novel polyelectrolyte poly(acrylic acid) grafted guar gum for adsorption of Pb(II) from acidic waste water. J Environ Chem Eng 4(2):1731–1742. https://doi.org/10.1016/j.jece.2016.02.034

57. Elhady S, Bassyouni M, Elshikhiby MZ, Saleh MY, Elzahar MH (2024) Advanced chitosan-based composites for sustainable removal of Congo red from textile wastewater. Discover Sustain 5(1). https://doi.org/10.1007/s43621-024-00349-5
58. Alcalde-Garcia F, Prasher S, Kaliaguine S, Tavares JR, Dumont M (2023) Desorption strategies and reusability of biopolymeric adsorbents and semisynthetic derivatives in hydrogel and hydrogel composites used in adsorption processes. ACS Eng Au 3(6):443–460. https://doi.org/10.1021/acsengineeringau.3c00022
59. Seo D, Park J, Shin TJ, Yoo PJ, Park J, Kwak K (2015) Bathochromic shift in absorption spectra of conjugated polymer nanoparticles with displacement along backbones. Macromol Res 23(6):574–577. https://doi.org/10.1007/s13233-015-3078-1
60. S C, H, U., S, S., H, K., D, S., J, T., N S (2022) Multi-Recyclable Eco-Friendly Chitosan Beads: an efficient adsorbent for removal of crystal violet dye. Austin Environ Sci 7(2). https://doi.org/10.26420/austinenvironsci.2022.1076
61. Miyah, Y., Ssouni, S., Benjelloun, M., El Addouli, J., Bouabadi, I., Jawhari, F.Z., … Lahrichi, A. (2024). Assessment of the Congo Red and Crystal Violet toxic dyes adsorption on chitin surface: response surface methodology optimization, regeneration,cost estimation, and phytotoxicity: Assessment of the Congo Red and Crystal Violet toxic dyes adsorption on chitin surface. *Moroccan Journal of Chemistry*, *12*(4), 1804–1824. https://doi.org/10.48317/IMIST.PRSM/morjchem-v12i4.51596
62. Li B, Shan C, Zhou Q, Fang Y, Wang Y, Xu F, Han L, Ibrahim M, Guo L, Xie G, Sun G (2013) Synthesis, characterization, and antibacterial activity of Cross-Linked Chitosan-Glutaraldehyde. Mar Drugs 11(5):1534–1552. https://doi.org/10.3390/md11051534

Figures

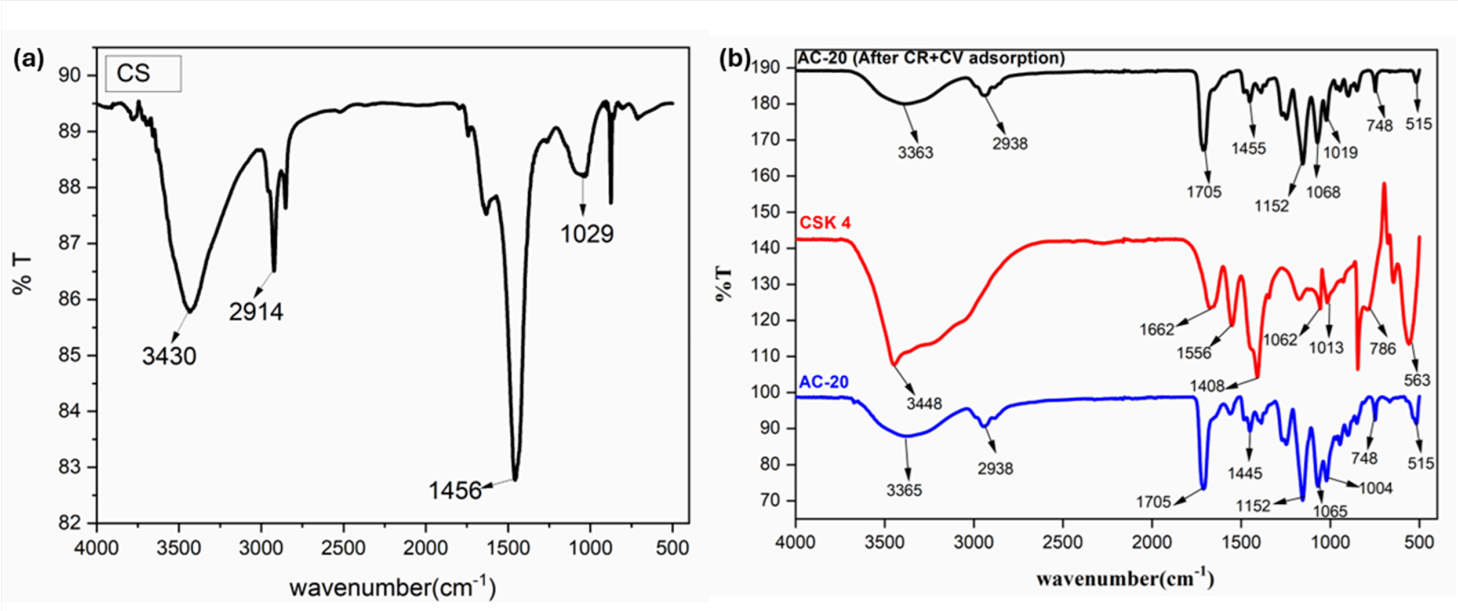


Figure 1

FTIR spectrum of (a) neat CS; (b) CSK-4, AC-20 (before and after dye adsorption)

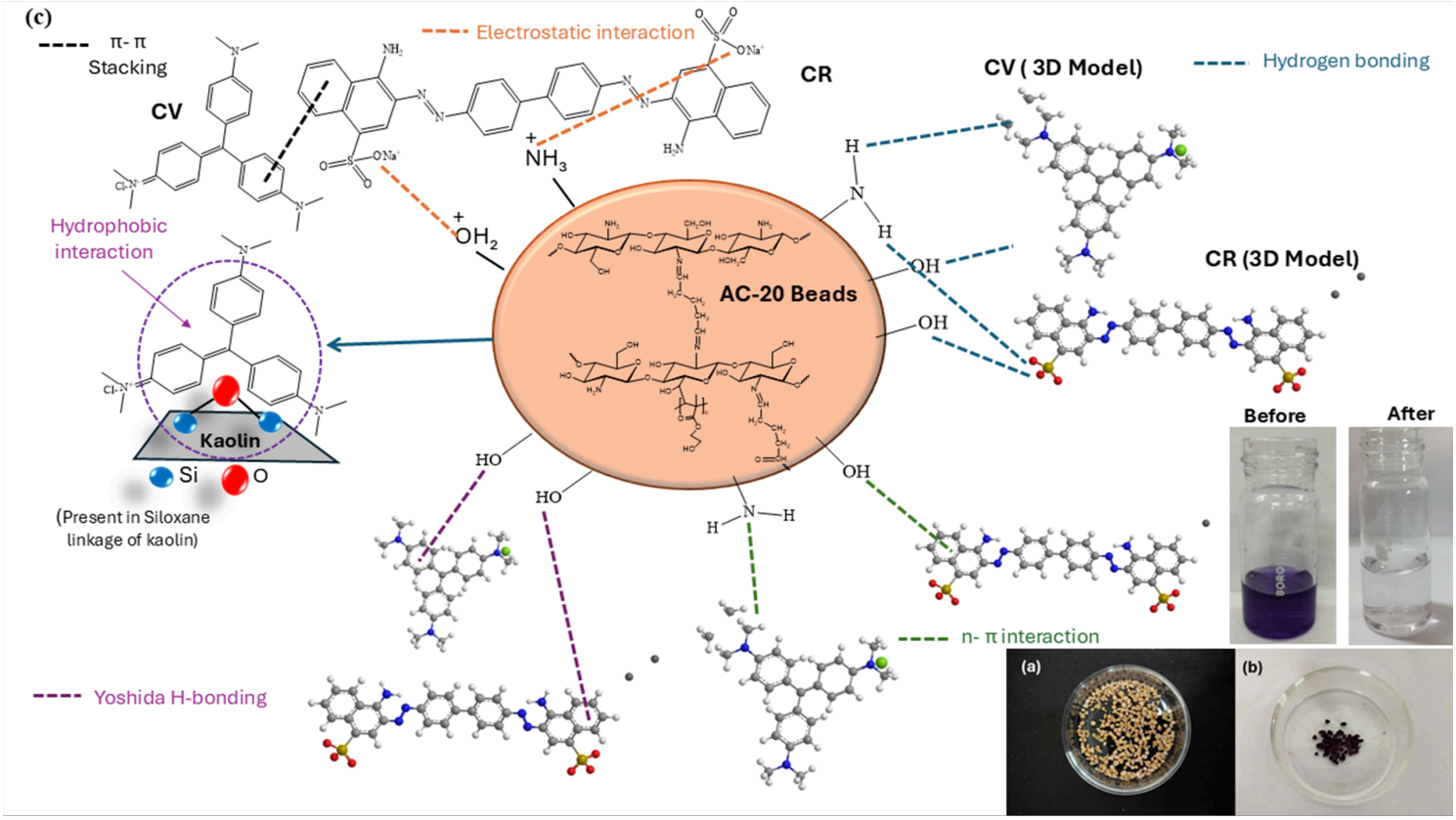


Figure 2

Photograph of AC-20 beads (a) before adsorption (b) after adsorption of CR and CV dyes (c) Adsorption mechanism between grafted beads with CR and CV dyes present in a binary mixture at pH=1

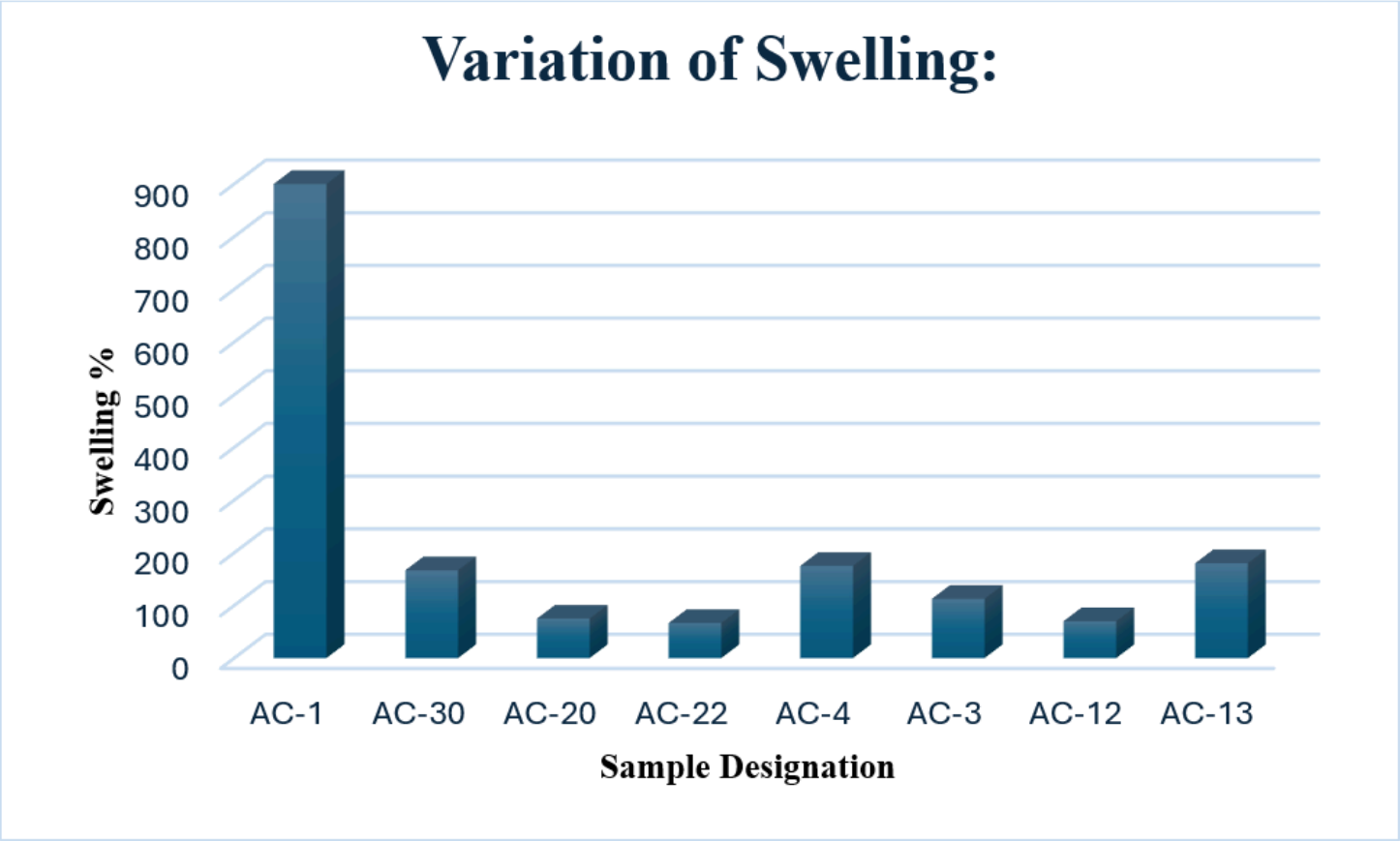


Figure 3

Bar Graph representing maximum swelling capacity by samples having variable kao, GL and HEMA content

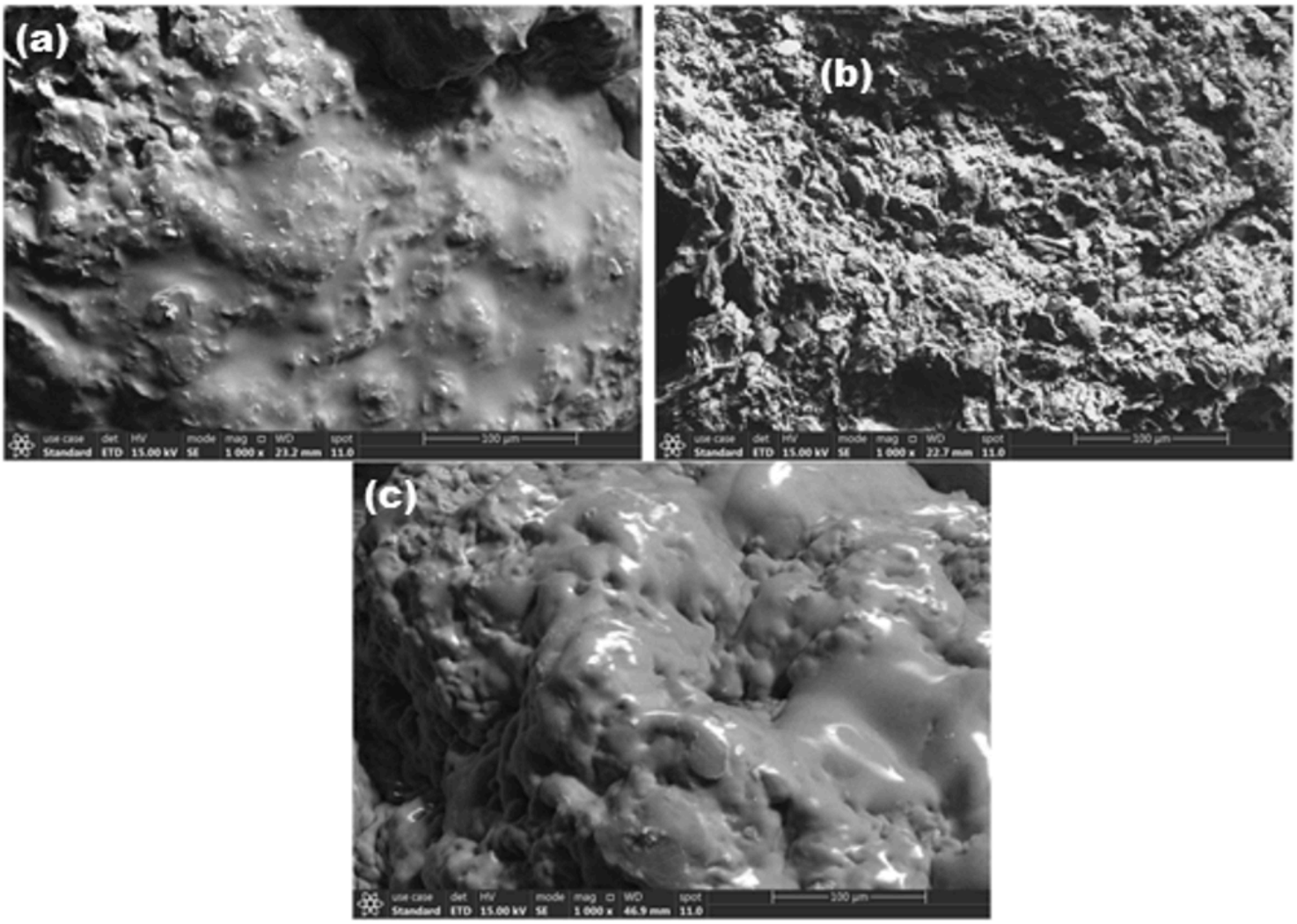


Figure 4

SEM images of (a): AC-20 beads with CS: Kao =1:1, (b): AC-22 beads with CS:Kao =1:2 and (c): AC-20 beads after adsorption of CR and CV dyes from their binary mixture.

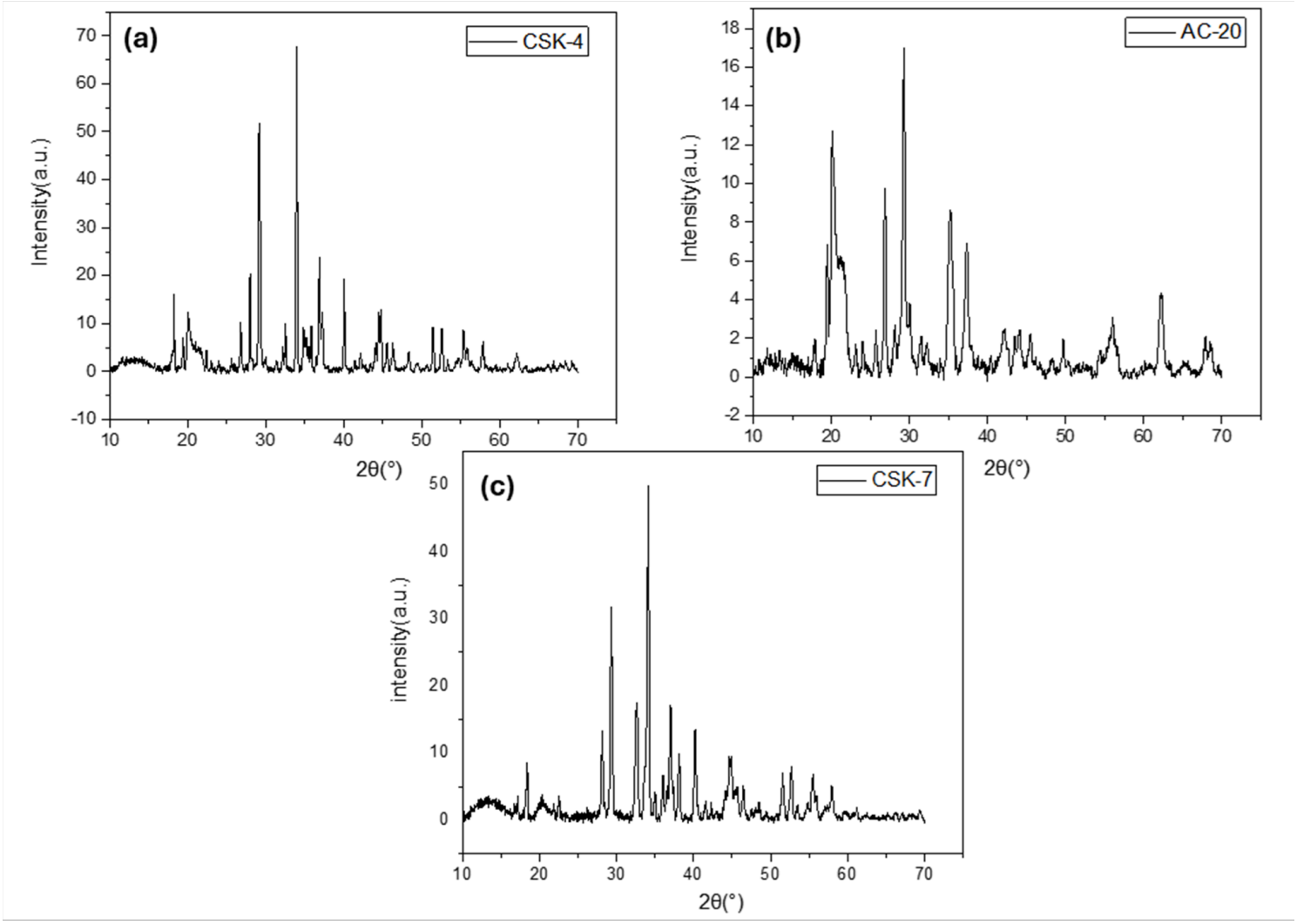


Figure 5

XRD patterns of (a)CSK-4 (b) AC-20 and (c) CSK-7

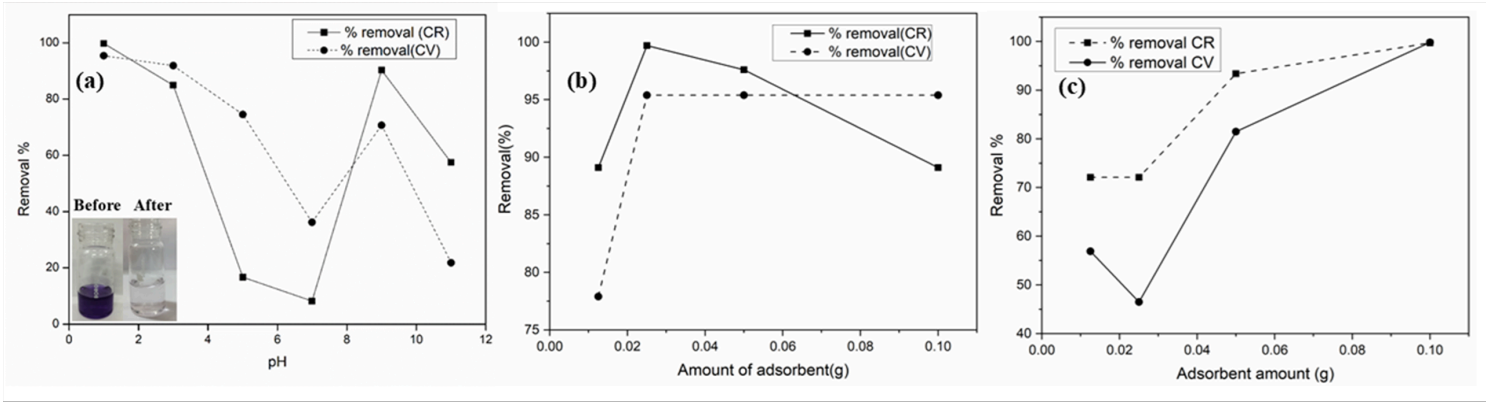


Figure 6

Effect of (a) pH, (b) adsorbent dosage of AC-20 and (c) adsorbent dosage of AC-22 on co-adsorption of Congo Red and Crystal Violet dyes from their binary mixture

Supplementary Files

This is a list of supplementary files associated with this preprint. Click to download.

- SupportingInformation.docx
- image1.tiff